5-2023

Generation and Characterization of a Multi-Functional Panel of Monoclonal Antibodies for SARS-CoV-2 Research and Treatment

Lila D. Patterson
Clemson University, lilap@g.clemson.edu

GENERATION AND CHARACTERIZATION OF A MULTI-FUNCTIONAL PANEL OF MONOCLONAL ANTIBODIES FOR SARS-CoV-2 RESEARCH AND TREATMENT

A Thesis
Presented to
the Graduate School of
Clemson University

In Partial Fulfillment
of the Requirements for the Degree
Master of Science
Microbiology

---

by
Lila D. Patterson
May 2023

Accepted by:
Dr. Charles D. Rice, Committee Chair
Dr. Vincent Gallicchio
Dr. Yanzhang Wei

ABSTRACT

The Coronavirus disease 2019 (COVID19) pandemic caused by SARS-CoV-2 is an ongoing threat to global public health. To this end, intense efforts are underway to develop reagents to aid in diagnostics, enhance preventative measures, and provide therapeutics for managing COVID-19. The recent emergence of SARS-CoV-2 Omicron strains with enhanced transmissibility, altered antigenicity, and significant escape of existing monoclonal antibodies and vaccines underlines the importance of the continued development of such agents. The SARS-CoV-2 spike protein and its receptor binding domain (RBD) are critical to viral attachment and host cell entry and are primary targets for antibodies elicited from both vaccination and natural infection. In this thesis research, mice were immunized with two synthetic peptides (Pep 1 and Pep 2) within the RBD of the original Wuhan strain of SARS-CoV-2, as well as the whole RBD as a recombinant protein (rRBD). Hybridomas were generated and a panel of three monoclonal antibodies, mAb CU-P1-1 against Pep 1, mAb CU-P2-20 against Pep 2, and mAb CU-28-24 against rRBD were generated and further characterized. The monoclonal antibodies were shown through ELISAs to be specific for each immunogen/antigen and to be reactive by immunoblotting against RBD. Monoclonal antibody CU-P1-1 has limited applicability other than in ELISA approaches and basic immunoblotting. Monoclonal antibody CU-P2-20 is very good for ELISAs, immunoblotting, and immunohistochemistry (IHC), but not live virus neutralization. In contrast, mAb CU-28-24 is very effective at live virus neutralization as well as ELISA, immunoblotting, and IHC. Moreover, mAb CU-28-24

was very active against rRBD proteins from Omicron variants B.2 and B.4/B5 as determined by ELISA, suggesting this mAb may neutralize live virus of these variants. Each of the immunoglobulin genes has been sequenced using Next Generation Sequencing, which allows the expression of respective recombinant proteins, thereby eliminating the need for long-term hybridoma maintenance. These hybridomas and related mAbs are now protected by Intellectual Property agreements with the Clemson University Research Foundation and are Patent Pending based on their unique amino acids within the complementary determining regions (CDRs).

DEDICATION

I would like to dedicate this thesis to Dr. Kristie Whitehead and Dr. John Abercrombie for introducing me to the field of microbiology, and for your constant support and encouragement over the years. To my friends and family, thank you for your love and kindness throughout this journey and for always being there for me. To my students, I have so enjoyed having the opportunity to teach you microbiology. I am so grateful for you all and thankful for all you have taught me. Lastly, I would like to dedicate this thesis to my late Aunt ML, whose love of science and education continues to inspire me.

ACKNOWLEDGMENTS

I want to acknowledge and thank my adviser, Dr. Charles D. Rice, for taking a chance on me and helping me to continue my education and grow as a scientist in and out of the lab throughout these past two years. I am so grateful for the opportunity to be a part of your lab, and to have had the chance to learn all that I have from you. I would also like to thank my “partner-in-crime”, Alyssa Whisel, for her friendship and assistance whenever I needed it. Thank you for putting up with me.

TABLE OF CONTENTS

Page

LIST OF FIGURES

BACKGROUND

Coronaviruses

Taxonomy and Classification

Coronaviruses (CoVs) are a large, highly diverse family of viruses belonging to the order *Nidovirales*, suborder *Cornidovirineae*, family *Coronaviridae,* and subfamily *Orthocoronavirinae*. Members of the *Coronaviridae* family are distinguished by spike-like projections extending from the viral envelope, giving the characteristic "crown-like" appearance for which they are named. The subfamily *Orthocoronavirinae* is composed of four genera categorized according to genome structure and phylogenic relationships: *Alphacoronavirus*, *Betacoronavirus*, *Gammacoronavirus,* and *Deltacoronavirus*. While alphacoronaviruses and betacoronaviruses exclusively infect humans and other mammals, gammacoronaviruses and deltacoronaviruses infect a broader host range, including avian species [1].

Genome and Virion Structure

Coronaviruses contain a non-segmented, positive-sense, single-stranded RNA genome with a 5' capped structure and 3'-poly-A tail [2]. Approximately two-thirds of the genome is occupied the two large open reading frames ORF1a and ORF1b, which are directly translated into the replicase proteins polyproteins pp1a and pp1b. These polyproteins are cleaved by virus-encoded proteases into 16 nonstructural proteins (nsp1-nsp16) to form the replication-transcription complex [3]. Downstream ORFs located near the 3'-terminus encode four main structural proteins: spike (S), membrane (M), envelope (E), and nucleocapsid (N) proteins. Interspersed within the structural genes are various

lineage-specific accessory genes nonessential to viral replication but thought to be involved in viral pathogenesis [2].

Coronavirus virions are roughly spherical with a diameter of approximately 80-120 nm. Homotrimers of the spike (S) protein project from the viral envelope to give CoVs their characteristic morphology. The type 1 transmembrane protein consists of an extracellular N-terminus, a transmembrane domain, and a short intracellular C-terminal segment. The ER-associated and heavily N-glycosylated S protein is divided into two functionally distinct subunits – the N-terminal S1 domain and the C-terminal S2 domain – responsible for receptor binding and membrane fusion, respectively [4]. The S-protein ordinarily exists in a metastable prefusion conformation, but undergoes extensive structural rearrangement upon viral interaction with the host cell receptor to facilitate membrane fusion and viral entry [2].

The coronavirus membrane (M) protein is the most abundant structural protein in the virion and is thought to play a major role in promoting membrane curvature contributing to the shape of the virion. The small M protein (~25-30 kDa) is an O-linked glycoprotein with a short N-terminal glycosylated ectodomain, three distinct transmembrane domains, and a larger C-terminal endodomain 6-8nm into the viral particle [2, 5]. Homodimeric M protein associates with E and N proteins to contribute to virion assembly and may also contribute to viral pathogenesis [6].

The envelope (E) protein (8-12 kDa) is found in small quantities within the coronavirus virion and is highly variable across CoVs. The transmembrane protein is involved in virion assembly and release, as well as additional functions beyond viral

replication. [2]. Acting as a viroporin, E assembles in membranes forming ion channels, influencing electrochemical balance in subcellular compartments, and contributing to pathogenesis [5].

The nucleocapsid (N) protein is solely responsible for the structural organization of the helical nucleocapsid. The structure of the nucleocapsid (N) protein is highly conserved, consisting of two separate domains capable of binding to RNA. Highly phosphorylated N protein homodimers and homoogliomers bind to the viral RNA genome, forming the ribonucleocapsid [5]. The N protein also binds to the key replicase complex component nsp3 and the M protein. In addition to contributing to viral assembly and budding, the protein is also involved in promoting cell-cycle arrest and inhibiting translation within the infected host cell [2, 5].

An additional structural protein, hemagglutinin-esterase (HE) is encoded by a subset of β-coronaviruses. The 48kDa glycoprotein forms homodimeric projections interspersed between spike homotrimers throughout the virion surface [5]. The HE protein acts as a hemagglutinin, binding sialic acid units on surface glycoproteins, while acetyl-esterase activity removes acetyl groups from O-acetylated sialic acids. It is thought that through these activities, HE is able to serve as a receptor-destroying enzyme, enhancing spike-protein mediated cell entry and viral spread through the mucosa [2]. HE expression is critical for infection in some β-coronaviruses, including the human coronavirus OC43 and bovine coronavirus (BCoV). Loss of HE esterase activity in OC43 inhibits both the production of infectious virus and viral dissemination in vitro. Similarly,

BCoV replication is blocked by acetyl-esterase inhibitors and neutralized by monoclonal antibodies against HE in vitro and in vivo.

Human Coronaviruses

To date, seven human coronaviruses (HCoVs) have been identified: HCoV-OC43, HCoV-HKU1, HCoV-NL63, HCoV-229E, severe acute respiratory syndrome coronavirus (SARS-CoV), Middle East respiratory syndrome coronavirus (MERS-CoV), and severe acute respiratory syndrome coronavirus 2 (SARS-CoV-2). Human coronaviruses (HCoVs) are associated with respiratory diseases of varying severity and are recognized as one of the most rapidly evolving groups of viruses due to high rates of genomic nucleotide substitution and recombination. The evolution of human coronaviruses has been expedited in recent years due to urbanization, deforestation, and farming practices, permitting species mixing and facilitating genomic recombination and crossing of species barriers by coronaviruses [7].

Human coronaviruses belong to the *alphacoronaviruses* (HCoV-229E and HCoV-NL63) or *betacoronavirus* (HCoV-OC43, HCoV-HKU1, SARS-CoV, MERS-CoV, and SARS-CoV-2) genera. While HCoVs share general characteristics of genome organization and viral life cycle, differences are found in receptor use, viral entry mechanisms, pathogenesis, and tissue tropism among other features observed between individual HCoVs [7]. All seven HCoVs have been found to be of zoonotic origin from bats, mice, or domestic animals. Available genomic analyses of HCoV support an

evolutionary origin of all human coronavirus from bats, while other species may serve as intermediate hosts [8].

Four HCoVs– HCoV-299E, HCoV-NL63, HCoV-OC43 and HCoV-HKU1– are endemic in the human population and distributed globally, contributing to approximately one-third of common colds annually. These 'common' coronaviruses are generally associated with mild self-limiting respiratory infections characterized by cough, fever, malaise, diarrhea, and rhinorrhea. In severe cases, these HCoVs can cause life-threatening pneumonia and lower respiratory tract infection in immunocompromised, elderly, and infant patients [7]. In the past two decades, three highly pathogenic HCoVs have emerged in the population: SARS-CoV in 2002, MERS-CoV in 2012, and SARS-CoV-2 in 2019. Unlike other HCoVs, these novel coronaviruses cause severe lower respiratory tract infections resulting in acute respiratory distress syndrome (ARDS), multi-organ failure, and septic shock with relatively high mortality.

SARS-CoV

SARS-CoV, the etiological agent of severe coronavirus (SARS), emerged in the Guangdong province of China in late November 2002. The highly transmissible SARS-CoV rapidly spread across 29 countries, resulting in 8,096 cases of SARS-CoV infection and 774 deaths (CFR = 9.6%). The outbreak was declared contained by the WHO in July 2003, with no reported cases of infection after May 2004. SARS-CoV is a lineage B betacoronavirus containing a positive-sense, single-stranded RNA genome 29.7kb in size. Host cell entry is mediated by binding of the receptor-binding domain located on the

SARS-CoV spike protein to the host receptor angiotensin-converting enzyme 2 (ACE2), with CD209 and CD209L functioning as co-receptors [9].

Retrospective epidemiological analysis revealed the majority of early SARS cases had a history of wild animal contact prior to the disease. Subsequent investigation into wild animal markets in Guangdong led to the isolation of a SARS-CoV-like virus from palm civets displaying a remarkably high similarity to SARS-CoV (99.8%). Within the wet market, approximately 80% of palm civets were serologically positive for SARS-CoV, while most wild civets and those raised on farms were SARS-CoV negative, indicating palm civets were likely intermediate hosts for SARS-CoV. A SARS-like coronavirus isolated from wild horseshoe bats, also present in Chinese wet markets, displayed 88-92% genomic identity to SARS-CoV [9]. These findings support the hypothesis that the virus first originated in bats as a result of multiple recombination events from a number of bat coronaviruses and was then transmitted to palm civets [10].

Initial symptoms of SARS-CoV infection typically include fever, cough, sore throat, dyspnea, headache, fatigue, and diarrhea. Disease progression is characterized by hypoxia, cyanosis, acute respiratory distress syndrome (ARDS), and multi-organ failure. Multifocal ground-glass opacities, consolidation, and interlobular septal thickening are commonly found upon chest imaging. Further pulmonary abnormalities include diffuse alveolar damage, extensive edema, alveoli collapse, and thrombosis [9]. The risk of severe disease is increased with age, the presence of comorbidities, and in males. Overall, 20-30% of patients with SARS require admission into intensive care units and subsequent mechanical ventilation. In the absence of effective and clinically approved antiviral

treatments, SARS patients primarily receive supportive care supplemented by various drug combinations, including ribavirin, IFNα, corticosteroids, and convalescent plasma therapy [3].

MERS-CoV

Middle East respiratory syndrome coronavirus (MERS-CoV) was first isolated from the sputum of a patient presenting with severe respiratory illness and renal failure in Jeddah, Saudi Arabia in June 2012 [11]. As of December 2022, 2603 laboratory-confirmed cases of MERS and 935 associated deaths (CFR = 36%) have been reported to the WHO across 27 countries, the majority of which were reported by Saudi Arabia (2194 cases and 854 deaths) [12]. MERS-CoV continues to circulate sporadically in the Middle East, causing community clusters and nosocomial outbreaks with potential global spread [13].

MERS-CoV is a lineage C *Betacoronavirus* with a single-stranded, positive-sense RNA genome 30.1-kb in length. Host cell entry is mediated by the binding of its S protein to the host receptor dipeptidyl peptidase 4 (DPP4). DDP4 is widely expressed on bronchial epithelial cells, type I and type II pneumocytes in the lung alveoli, as well as epithelial cells of the kidneys, liver, and intestines [13]. Similarly, to SARS-CoV, MERS-CoV is thought to have originated from bats. PCR amplification of nucleic acid isolated from bat stool revealed 100% nucleotide identity with MERS-CoV from an infected patient in the same area. Phylogenetic analysis clusters MERS-CoV to the same group as several bat coronaviruses, further supporting the role of bats as a natural reservoir. MERS-CoV has also been isolated from dromedary camels in the middle east, with

serological evidence of the circulation of MERS-like viruses in dromedary camels dating back to 1983. Transmission from camels to humans primarily occurs through respiratory droplets and the fecal-oral route of transmission [8]. Human-to-human transmission primarily occurs in healthcare facilities, accounting for approximately half of all cases reported to the WHO [12, 13]. The frequency of nosocomial transmission is thought to be a result of the significant viral shedding that occurs following symptom onset when medical care is most often sought out. In the healthcare setting transmission of MERS-CoV most frequently occurs between patients and from infected patients to healthcare workers [13].

The incubation period of primary MERS infections remains unknown, though data from cases of human-to-human transmission estimate the incubation period to be between 5-7 days. Clinical presentation of infected individuals ranges from asymptomatic or mild respiratory illness to severe, with an overall morbidity rate of 36% [14]. Initial symptoms of MERS include fever, chills, cough, malaise, headache, dyspnea, and myalgia. Gastrointestinal symptoms such as nausea, vomiting, abdominal pain, and diarrhea preceding the development of pneumonia occur in some patients. Abnormal chest x-ray and CT findings are common in MERS patients (90-100%). These abnormalities include diffuse bilateral ground-class opacities, pleural effusion, consolidation, interstitial infiltrates, and bronchiolar wall thickening. Up to 50% of symptomatic adults require admission to intensive care units, with up to 70% of these patients requiring mechanical ventilation [13, 14]. Disease complications include respiratory failure, acute respiratory distress syndrome (ARDS), septic shock, and

multiorgan failure. Severe disease is more likely in those older than 60 years, immunocompromised patients, and those with chronic comorbid diseases such as liver, heart, and kidney disease.

To date, there are no approved vaccines or therapeutics for the prevention and treatment of disease caused by MERS-CoV. The management of MERS patients is primarily supportive and symptom-focused, typically aiming to prevent or treat secondary infections and reduce the risk of other complications, such as respiratory and renal failure [15]. Several treatments have been empirically studied in patients with severe disease, including convalescent plasma, antiviral agents such as interferons and ribavirin, corticosteroids, and protease inhibitors. The efficacy of these treatments, however, is unknown due to the absence of controlled clinical trials.

SARS-CoV-2

Origin and Evolution

In late December 2019, several clusters of atypical pneumonia of an unknown etiology were reported in Wuhan, China. Patients presented with symptoms of viral pneumonia, including fever, cough, dyspnea, and bilateral lung infiltration. Additionally, most patients were found to be epidemiologically linked to the Huanan Seafood Wholesale Market, a large wet market in Wuhan selling a large variety of different live wild animals. In January 2021, the complete genome sequence of the novel virus was obtained from samples collected from five hospitalized patients with atypical pneumonia in Wuhan, China. Bioinformatic analysis revealed the etiological agent, later named SARS-CoV-2, to be a novel lineage 2B betacoronavirus, with 79.5% sequence identity to

SARS-CoV [16]. Alignment of the SARS-CoV-2 genome against that of other betacoronavirus indicated SARS-CoV-2 to be most closely related to the SARS-like BatCoV RaTG13 with an identity of 96%. These findings suggest SARS-CoV-2 to have most likely originated from bats, having naturally evolved from RaTG13. SARS-like coronavirus isolated from Malayan pangolins within the market demonstrated up to 99% sequence similarity to SARS-CoV-2 and 90.55% identity to BatCoV RaTG13 [17, 18]. Further, the viral genes E, M, N, and S display a remarkably high genetic similarity between SARS-CoV-2 and the Pangolin SARS-like coronavirus at 100%, 98.6%, 97.8%, and 90.7%, respectively [16].

Epidemiology and Transmission

As of March 16, 2023, over 760 million confirmed cases and 6.8 million deaths globally have been reported to the WHO. The reported counts and current trends underestimate the true number of cases and associated deaths, as shown by prevalence surveys, likely due to undiagnosed infections, reductions in testing, and delays in reporting [19]. Early epidemiological monitoring provided estimates the viral reproduction number (R_0) of the parental (Wuhan) strain of SARS-CoV-2 between 2.2-2.9, with a doubling time of 5 days [17]. The R_0 value of SARS-CoV-2 indicates the virus is more transmissible than SARS-CoV, likely due to differences in the SARS-CoV-2 receptor binding domain that enhance binding affinity to the host receptor ACE2 [20].

The primary route of SARS-CoV-2 transmission is via respiratory droplets during unprotected close contact with an infected individual. Additionally, the occurrence of aerosol transmission is well-reported in crowded, poorly-ventilated indoor settings and

within hospitals, where aerosol-generating procedures such as respiratory therapies are common [20]. In contrast to SARS-CoV-2, asymptomatic and pre-symptomatic transmission is common and is thought to contribute to a significant number of infections [21].

Clinical Characteristics

SARS-CoV-2 infection is associated with a broad range of symptoms and clinical outcomes ranging from asymptomatic to critical and potentially life-threatening illnesses. Symptom onset typically occurs following an incubation period of 3-5 days and is most commonly marked by fever, cough, fatigue, loss of taste or smell, and myalgia [17]. Less common symptoms include diarrhea, loss of taste or smell, chest discomfort, sore throat, and anorexia [22]. Asymptomatic infection is well-documented and is estimated to occur in 40.5% of infected individuals [23]. Of symptomatic patients, most patients develop only mild symptoms with or without mild pneumonia (81%). The development of severe and critical disease occurs in 14% and 5% of patients, respectively [3]. Increased risk of severe disease is observed in older individuals and those with pre-existing comorbidities, including immunosuppression, hypertension, diabetes, obesity, heart disease, kidney disease, and chronic lung diseases such as asthma and COPD [17].

In COVID-19 patients, bilateral ground-glass opacities, shadowing, and consolidation in the lungs are typical upon CT scan. Additional pathological findings include the presence of proteinaceous exudates in lung tissues, the development of pulmonary edema, interstitial thickening, bilateral diffuse alveolar damage, and infiltration of immunocytes. Plasma concentrations of IL-2, IL7, IL-10, TNFα , GSCF

are increased in severe and critical patients and is associated with mortality [3]. Extrapulmonary manifestations include myocardial injury, arrhythmia, impaired consciousness, acute kidney and liver injury, thrombosis, and stroke. Critical patients may require mechanical ventilation or extracorporeal membrane oxygenation (ECMO) rapidly progress to acute respiratory distress syndrome (ARDS), respiratory failure, septic shock, and multi-organ failure, and death [16]. Most COVID-19 infections do not require hospitalization, typically resolving within two weeks. Non-hospitalized patients with mild to moderate covid who are at risk of progression to severe disease may be prescribed antiviral medication, such as Paxlovid or Remdesivir. Antiviral medication is typically combined with the corticosteroid dexamethasone and immunomodulators (IL-6 inhibitors, JAK inhibitors) [24]

Most COVID-19 infections do not require hospitalization, typically resolving within two weeks. Non-hospitalized patients with mild to moderate covid who are at risk of progression to severe disease may be prescribed antiviral medication, such as Paxlovid or Remdesivir. Antiviral medication is typically combined with the corticosteroid dexamethasone and immunomodulators (IL-6 inhibitors, JAK inhibitors) [24].

Genome Organization

SARS-CoV-2 is a lineage 2B betacoronavirus consisting of a single-stranded, positive-sense RNA genome 29.9 kb in size. The SARS-CoV-2 genome is flanked by a 5’ methylated cap and a 3’-polyadenylated tail, and consists of two untranslated regions (UTRs) located at the 5’ and 3’ ends and 14 open reading frames (ORFs) encoding 27 proteins [21]. The 5’ methylated cap and 3’-polyadenylated tail allow the positive-sense

RNA genome to be directly translated by the host cell upon entry [25]. The first ORF (ORF1a/b) comprises approximately two-thirds of the genome, encoding 16 non-structural proteins essential to viral replication. The remaining one-third of the genome encodes four structural proteins S, M, E, and N, and at least six accessory proteins [21].

Spike Glycoprotein

SARS-CoV-2 host cell entry is mediated by the highly glycosylated spike (S) protein trimers that span the surface of the viral envelope. The spike protein is a type 1 transmembrane N-linked glycosylated protein recognizing the host cell receptor angiotensin-converting enzyme 2 (ACE2). Following receptor binding, the SARS-CoV-2 S protein is cleaved by the host membrane proteases TMPRSS2 and furin into two functional subunits, S1 and S2, which remain associated. Upon entry, the SARS-CoV-2 RNA genome is directly translated into polyproteins by the host cell ribosomes, and viral replication and transcription occur via cleavage of the polyprotein by viral proteases and assembly of the replicase-transcriptase complex. Viral components are then assembled and packaged into new virions to be released from the host cell [4].

The S protein is 1273 amino acids in length, consisting of an N-terminal signal peptide (amino acids 1-13) and the two functional subunits S1 (14-685 residues) and S2 (686-1273 residues), responsible for host cell attachment and membrane fusion, respectively. In the prefusion conformation, the SARS-CoV-2 S protein exists an inactive precursor [3]. Following receptor binding, the host membrane proteases TMPRSS2 and furin cleave the S protein into two subunits, S1 and S2, inducing conformational changes facilitating membrane fusion and host cell entry [25]. The S1 domain contains the N-

terminal domain (NTD, 14-305 residues), and the receptor binding domain (RBD, 319-541 residues). The S2 subunit is comprised of heptapeptide repeat sequence 1 (HRP1, 912-984 residues), HR2 (127-1213 residues), a transmembrane domain (1213-1237), and a short cytoplasmic domain (1237-1273) [4].

Monoclonal Antibodies and SARS-CoV-2

Owing to their high specificity and reliability, monoclonal antibodies (mAbs) targeting antigenic regions of viral surface proteins are highly valuable agents for the detection, treatment, and prevention of diseases. The urgent need for such tools has prompted the rapid development of a vast number of monoclonal antibodies targeting SARS-CoV-2.

As of June 2022, five anti-SARS-CoV-2 monoclonal antibodies received emergency use authorization (EUA) from the FDA for the treatment and prevention of COVID-19 in non-hospitalized patients at high risk for severe disease. All monoclonal antibodies previously granted EUA are directed against the SARS-CoV-2 S protein, inhibiting the interaction between the RBD and ACE2 and blocking viral entry and infection. Clinical trials showed SARS-CoV-2 neutralizing monoclonal antibodies to be safe and well tolerated, and early administration of was found to reduce the risk of disease progression by up to 80% [26]. When given to asymptomatic individuals, monoclonal antibody treatment was found to reduce the incidence of symptomatic infection and was also shown to be effective in the prevention of disease or infection in those exposed to SARS-CoV-2 [26]. The emergence of SARS-CoV-2 variants, most notably Omicron and Omicron subvariants, resulted in significant escape and resistance

against previously effective vaccines and monoclonal antibodies [26]. As a result, no available monoclonal antibodies are currently approved for the treatment and prevention of COVID-19. The continued development of monoclonal antibodies against SARS-CoV-2 is essential for continued efforts to control the spread of COVID-19 and combat current and future variants.

INTRODUCTION

The SARS-CoV-2 virus and associated severe pneumonia first appeared in the Wuhan Province of China in late 2019, and within weeks had spread globally to what is now known as the COVID-19 pandemic [27]. Early epidemiological monitoring provided estimates the SARS-CoV-2 reproduction number (R_0) of the parental (Wuhan) strain of SARS-CoV-2 between 2.2-2.9, with a doubling time of 5 days [17]. The R_0 value of SARS-CoV-2 indicates the virus is more transmissible than SARS-CoV, likely due to differences in the SARS-CoV-2 receptor binding domain that enhance binding affinity to the host receptor ACE2 [20]. The primary route of SARS-CoV-2 transmission is via respiratory droplets during unprotected close contact with an infected individual. Additionally, the occurrence of aerosol transmission is well-reported in crowded, poorly ventilated indoor settings and within hospitals, where aerosol-generating procedures such as respiratory therapies are common [20]. In contrast to SARS-CoV-2, asymptomatic and pre-symptomatic transmission is common and is thought to contribute to a significant number of infections [21].

Most COVID-19 infections do not require hospitalization, typically resolving within two weeks. Non-hospitalized patients with mild to moderate disease who are at risk of progression to severe disease may be prescribed one of the three antiviral medications: oral nirmatrelvir *(Paxlovid)*, intravenous remdesivir *(Veklury)*, and oral molnupiravir *(Lagevrio)*. Paxlovid is FDA-approved for such use, but the other two are only available under the Emergency Use Authorization [28-32]. Antiviral medication is

typically combined with the corticosteroid dexamethasone and immunomodulators (IL-6 inhibitors, JAK inhibitors).

Monoclonal antibodies (mAbs) targeting antigenic regions of viral surface proteins are highly valuable agents for the detection, treatment, and prevention of disease progression. The urgent need for such tools has prompted the rapid development of a vast number of monoclonal antibodies targeting SARS-CoV-2. In convalescent patients and in individuals post vaccination, most of the circulating IgG antibodies are against S1 epitopes outside of the receptor binding domain, and these are typically not neutralizing antibodies [33]. In contrast, most SARS-CoV-2 neutralizing antibodies are generated against the RBD [34, 35]. As of June 2022, five anti-SARS-CoV-2 monoclonal antibodies received emergency use authorization (EUA) from the FDA for the treatment and prevention of COVID-19 in non-hospitalized patients at high risk for severe disease [36]. All monoclonal antibodies previously granted EUA are directed against the SARS-CoV-2 S1, including the RBD protein, inhibiting the interaction between the RBD and ACE2 and blocking viral entry and infection. Clinical trials showed SARS-CoV-2 neutralizing monoclonal antibodies to be safe and well tolerated, and early administration of was found to reduce the risk of disease progression by up to 80% [26]. When given to asymptomatic individuals, monoclonal antibody treatment early in the pandemic was found to reduce the incidence of symptomatic infection and was also shown to be effective in the prevention of disease or infection in those exposed to SARS-CoV-2 [26].

The continued development of monoclonal antibodies against SARS-CoV-2 RBD is essential for continued efforts to control the spread of COVID-19 and combat current

and future variants. However, since the evolution of Omicron strains most approved mAbs for COVID-19 therapy no longer demonstrate efficacy in mitigating the clinical progression of disease [37]. One mAb, Bebtelovimab, originally held promise as it neutralized very early Omicron variants of concern, but has become less effective due to the evolution of newer, more resistant strains [38]. Despite rapid advances in the development of therapeutics for SARS-CoV-2-related pathologies, there remains the need for monoclonal therapeutics targeting recent (and future) variants of concern.

To date, most efforts to develop mAb therapies for COVID-19 are focused on neutralizing antibodies [39], though mAbs have many other properties and applications. For example, an antibody may lack the ability to neutralize the SARS-CoV-2 virus, but may well recognize epitopes revealed during ELISA applications, immunoblotting, and immunohistochemistry. Likewise, mAbs that may have limited use in these areas may be very good neutralizing antibodies. In the study described herein, a simplified adaptation of current COVID-19 vaccines based on spike mRNA or insect cell expression of recombinant spike proteins were used to generate a panel of mAbs. These mAbs were used to test the hypothesis that immunogenic synthetic peptides (15 – 20 amino acids) can induce the production of high quality mAbs for multiple applications in SARS-CoV-2 research and treatments. Specific immunogenic synthetic peptides derived from the receptor binding domain region of spike proteins were conjugated to a large carrier protein (keyhole limpet hemocyanin; KLH) and used to immunize mice for the generation of polyclonal anti-sera and mAbs and compared to antibodies generated because of immunizations with whole recombinant RBD protein. These were then tested

for their ability to neutralize the original Wuhan strain of SARS-CoV-2 and recognize the RBD by ELISA, immunoblotting, and immunohistochemistry. One mAb, mAb CU-28-24, not only neutralizes the original Wuhan strain, but is also highly cross reactive against recent Omicron variants BA.2 and BA.4.5.

MATERIALS AND METHODS

Immunogen design

Synthetic peptides within two internal amino acid sequences (between 400 – 500) of the receptor binding domain (Arg319 – Phe541) of the original Wuhan strain of SARS-CoV-2 spike protein were designed from a full-length RBD cDNA sequence (accession # NC_045512.2) and conjugated with keyhole limpet hemocyanin (KLH) (Anaspec, Richmond CA) for immunizations and as unconjugated peptide for screening assays. The actual sequence of the peptides is proprietary information. Recombinant RBD (Arg319 – Phe541) of the same strain was obtained from Invitrogen (# RP 87678) and used as an immunogen without conjugation with KLH and used for screening assays. Sequences of the two synthetic peptides were chosen based on Hopp-Woods hydrophilicity profiles (https://web.expasy.org/protscale/), NIH-Ab-designer algorithms (https://esbl.nhlbi.nih.gov/AbDesigner/), peptide solubility (http://pepcalc.com/), and the differential homology between SARS-CoV-2 and SARS-CoV-1, or other coronaviruses (https://blast.ncbi.nlm.nih.gov/Blast.cgi). These peptide sequences were then checked for possible negative internal amino acid interactions prior to final selection.

Polyclonal and monoclonal antibody generation

Six-week-old female Balb/c mice (Charles River) were used for immunizations and housed at the Godley Snell Animal Facility, a Clemson University IACUC approved facility under an IACUC-approved protocol (AUP2020-0069). Mice were given a sub-cutaneous (s.c.) injection with 100 μg of immunogen in 0.9% saline containing TiterMax

Gold® adjuvant on Day 1. Fourteen days later mice received a second s.c. immunization using Freund's incomplete adjuvant. Subsequent boosters at 21-day intervals were given in saline via s.c. immunizations, and the final booster was given intraperitoneally. Five days after the last booster immunization, mice were sacrificed using slow lethal CO_2 hypoxia, bled by cardiac puncture at the time of pneumothorax detachment to collect polyclonal anti-sera, and their spleens removed using aseptic methods. Procedures for fusion of splenocytes with Sp02–14 myelomas (ATCC, Manassas VA USA), and for screening and cloning of the resulting hybridomas have been described elsewhere [40-42]. Hybridomas were typically grown in Dulbecco's Modified Eagle Medium (Cellgro) supplemented with 10% fetal bovine serum (FBS), 20 mM HEPES, 10 mM L-glutamine, 100 µg/mL penicillin, 100 µg/mL streptomycin, 110 µg/mL sodium pyruvate, 1% non-essential amino acids (100× stock), 4.5 g/L glucose, 10 µg/mL gentamycin and 5 µg/mL nystatin. Blood samples were allowed to clot, then centrifuged to collect overlying serum to serve as anti-sera in subsequent assays.

Primary hybridoma supernatants were then screened by ELISA against unconjugated peptide (2 µg/well) or rRBD (2 µg/well). Briefly, immunogens were diluted to 20 µg/ml in 0.01 M phosphate buffered saline, pH 7.2 (PBS) and 100 ul added to wells of a 96-well medisorp ELISA plate (Thermo Fisher Scientific #467320) and incubated overnight at 4º C. Plates contents were then discarded, and plates washed 5X with PBS containing 0.01% Tween-20 (PBST). Plate wells were then blocked overnight with 150 µl of PBS containing 10% horse serum (blocking buffer). Plate contents were then discarded, and plates received 100 µl of hybridoma supernatant, followed by

incubation at room temperature for 2 hours. Plates were washed 5X with PBST, then received 100 µl goat anti-mouse IgG-AP (Thermo Fisher 1:2000 in PBS) and incubated for 2 hours at room temperature. Finally, the plates were washed 5X with PBST, then received 100 µl of *p*-nitrophenyl phosphate substrate in alkaline phosphatase buffer (100 mM NaCl, 50 mM $MgCl_2$, 100 mM Tris-Cl, pH 9.5) (AP). After 30 minutes,the plates received 100 µl of stopping buffer (2 M NaOH) and were read at 405 nm and the optical density recorded.

Cells from wells with a minimal signal of three-fold optical density readings above the lowest reading wells were then cloned by limiting dilution for further testing. Hybridomas were grown to confluence and the supernatants collected by centrifugation, then treated with 0.05% NaN_3 and stored at 4°C. Initial isotyping of the antibodies in hybridoma supernatants was carried out using Pierce Rapid Antibody Isotyping Kits for mouse (Thermo Fisher). Antibodies were subsequently used as confluent supernatants for most techniques, or further purified over protein A/G columns as needed. For obtaining purified mAbs, the hybridomas were grown in complete media as described above but containing ultralow bovine IgG serum (Fisher Scientific) to avoid purifying bovine IgG over mouse IgG. Preliminary studies demonstrated that only three hybridomas secreted antibodies specific to the immunizing peptides or rRBD. Of these, one secreted an antibody (mAb CU-P1-1) that recognizes pep-1 by ELISA, one that secreted an antibody (mAb CU-P2-20) against pep-2, and one (mAb CU28-24) that recognizes the rRBD. Immunoglobulin (Ig) genes of the three hybridomas were then sequenced (Absolute Antibody/Kerafast, Boston MA USA) using Next Generation

Sequencing (NGS) to verify the presence of a single Ig and of the appropriate isotype. The unique complimentary determining region (CDR) sequences of heavy and light chains have been determined, and these Ig sequences will allow for the expression of recombinant mAbs.

Screening polyclonal anti-sera and mAbs for reactivity against rRBD.

Stored rRBD was diluted in PBS to 100 ug/ml, mixed with 6X reducing sample buffer (SB), and boiled for 7 minutes. Protein molecular weight markers (FroggoBio, Buffalo NY, USA) and 2 ug of rRBD were subjected to SDS-PAGE using 4-20% gels, then transferred to PVDF membranes. Membranes were then blocked overnight with blocking buffer, washed 3X with PBST, and then probed with the three polyclonal anti-sera samples diluted 1:500 in PBS, or the three mAbs as confluent supernatants diluted 1:3 in PBS (nominal concentration of 3 μg/ml), followed by washing 3X with PBST. The blots were then probed with goat-anti-mouse IgG-AP (Themofisher, 1:2000 in PBS) for 2 hours at room temperature, washed 3X with PBST, then developed using the substrate BCIP/NBT (Fisher Scientific) to detect the protein of interest as a dark blue band. The development process was stopped by extensive washing with tap water, the blots dried at room temperature, then imaged using a ChemiDoc™ imaging system (Biorad).

Screening mAbs for specificity

To determine the specificity of mAbs, ELISA plates were again coated with unconjugated peptides or rRBD. Using the above-described ELISA approaches, each

polyclonal anti-sera sample diluted 1:250 in PBS and mAb as confluent supernatants diluted 1:3 in PBS were used as primary antibody against peptide 1, peptide 2, or rRBD. An irrelevant mAb was used as an assay control [43]. After development, the optical density of each well was recorded at 405 nm to compare the reactivity of each mAb with each antigen.

Immunoprecipitation of rRBD with CU28-24.

From the immunoblots and ELISA data it was determined that mAb CU28-24 is specific for the native rRBD protein but does not recognize the protein under the denaturing conditions of SDS-PAGE and immunoblotting. To further validate that mAb CU-28-24 is specific for rRBD, but not recognizing either of the epitopes recognized by mAb CU-P1-1 or CU-P2-20, purified mAb CU-28-24 was applied to a protein A/G column by running the sample over the column 3X. The column was washed extensively with PBS, followed by the addition of 100 ug rRBD in 3 ml PBS which was reapplied to the column 3X. Next the column was washed 4X with 4 ml PBS, and the wash steps collected. After the final wash, proteins associated with the column were eluted with 0.8 ml aliquots of 0.05 M glycine, pH 2.5 and collected in tubes containing 0.2 ml of carbonate buffer, pH 9. These samples and wash samples were then mixed with SB and boiled, then subjected to SDS-PAGE and immunoblotting. One lane of the gel contained 2 ug of rRBD as a positive control. The blots were blocked overnight with PBS containing 10% horse serum, washed 3X, then probed with FITC conjugated [44] purified mAb CU-P2-20 diluted in PBS to 5 μg/ml. The blot was washed 3X, dried, and imaged for fluorescent banding using a ChemiDoc™ imaging system (Biorad).

SARS-CoV-2 surrogate virus neutralization assays.

A commercially available kit to quantify the ability of the three pAbs and 3 mAbs to neutralize the binding of RBD to ACE-2 was obtained from GenScript, Piscataway NJ (kit #L00847). The methods followed those provided by the supplier. The wells were precoated by the manufacturer with rACE-2 protein. In brief, pAb samples were diluted 1:10, 1:50, 1:100, and 1:200 in assay dilution buffer, and purified mAbs were diluted to 50 ug/ml in PBS, and further diluted in assay dilution buffer to yield 2.5, 1.8, 0.6, and 0.2 ug per well in the provided assay ELISA plate. Diluted samples (pAbs and mAbs) and HRP-labeled RBD were mixed, incubated as directed, and then applied to the ACE-2-coated plate in duplicates. After 30 minutes incubation, the plates were washed extensively with provided wash buffer, and HRP substrate was added. After 30 minutes the reaction was stopped with provided stop buffer and the optical density at 450 nm was recorded and the data was processed as directed by the manufacturer and expressed as percent signal inhibition. Positive and negative control anti-sera solution were provided by the manufacturer.

Plaque reduction neutralization test (PRNT) assays

Virus neutralization assays were carried out at Georgia State University under the supervision and generosity of Dr. Mukesh Kumar using a certified Animal Biosafety Level 3 laboratory under an approved IACUC protocol (AUP-A20044). The details of PRNT follow standard protocols [45]. The three mouse mAbs were diluted to 50 μg/ml in PBS to begin the test. Vero6 cells were used as the host target model and live SARS-CoV-2 strain USA-WA1/2020 virus was used for infection.

Tissue Immunohistochemistry

Brain and lung tissues from infected and control mice were a generous gift from Dr. Mukesh Kumar, Georgia State University. In brief, hemizygous K18-hACE2 mice were purchased from the Jackson Laboratory (Bar Harbor, ME) and animal experiments were conducted in a certified Animal Biosafety Level 3 (ABSL-3) laboratory at Georgia State University (GSU) under the direction of Dr. Mukesh Kumar as previously described [46]. Six-week-old hemizygous K18-hACE2 mice were infected with 10^5 plaque-forming units (PFU) of SARS-CoV-2 strain USA-WA1/2020 under ABSL-3 containment by intranasal inoculation. Animals in the control group received equivalent amounts of sterile PBS via the same route. Mice that met the human endpoint criteria were euthanized to limit suffering. Animals were then perfused with 10 ml PBS via cardiac puncture, followed by perfusion with 10 ml 4% paraformaldehyde. Lungs and brains were grossed, recorded, and then were placed in 10% buffered formalin. After three days, the formalin was removed and replaced with 70% ethanol for storage.

Tissues were processed and embedded in ParaPlast Extra by the Louisiana Animal Disease Diagnostic Laboratory (LADDL) at Louisiana State University School of Veterinary Medicine. Newly embedded tissues were then sectioned and affixed to charged slides for H&E staining and immunohistochemistry. For antigen retrieval, tissue slices were microwave-heated in either pH 6 citrate buffer or pH 9 Tris-EDTA. Tissues were then encircled with a Liquid Blocker Super mini pen to isolate tissue slices, thus dividing each slide into two sections to allow one section to act as a reagent control by withholding primary antibody treatment. Additional screening assays included isotype

controls. All sections were subsequently blocked with 5% horse serum (VectaStain®) blocking buffer for 17 minutes. Next, the antibody, as hybridoma supernatant diluted 1:3 in PBS with 1.5% horse serum, was added dropwise to the slides and incubated overnight at 4 °C. After incubation, the slides were washed prior to addition of the secondary antibody (goat anti-mouse IgG-Alexafluor488, 5 ug/ml, Invitrogen) and incubated for 2 hours at room temperature. Slides were washed 5X in PBST, stained with DAPI for 5 min, washed again. Finally, slides were mounted, cover-slipped and imaged.

Screening polyclonal anti-sera and mAbs for reactivity against Omicron BA.2 and BA.4.5 variant rRBDs.

Recombinant Omicron RBD proteins from variants BA.2 and BA.4.5 were obtained from Fisher Scientific. To determine the specificity of mAbs, ELISA plates were coated with rRBD from the two variants as well as from the original Wuhan strain. Using the above-described ELISA approaches, each mAb as confluent supernatants diluted 1:3 in PBS were used as primary antibody. After development, the optical density of each well was recorded at 405 nm to compare reactivity of each mAb with each antigen.

RESULTS

Immunizations and resulting anti-sera.

In this study, mice were immunized with two different synthetic peptides mapping to the RBD region of the SARS-CoV-2 spike protein. Mice were also immunized with commercially available rRBD expressed in HEK cells. The product is approximately 37 kDa (Figure 1). This product, like most recombinant proteins, tends to degrade slightly upon thawing and refreezing.

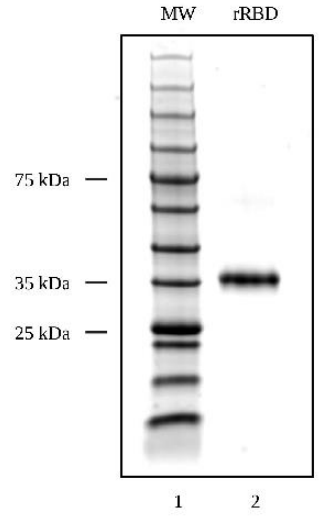

Figure 1. SDS-PAGE and Coomassie blue staining of SARS-CoV-2 (Wuhan) recombinant RBD used for immunizations and antibody screening. SDS-Page and Coomassie blue staining of rRBD protein. Lane 1: 12 ul protein molecular weight marker. Lane 2: 2 µl of 37 kDa rRBD protein.

Serum from mice immunized with peptides and whole rRBD was used as a source of anti-sera to determine if mice responded immunologically to the immunogen associated with RBD. Anti-sera from all three immunogens recognized rRBD by

Western blots (Figure 2). In each case, the partially degraded rRBD product was also recognized by the respective anti-sera. Anti-sera were also used to determine the degree of specificity against the respective peptide and rRBD by ELISA. Anti-sera from mice immunized with peptide 1 (P1) recognized P1, but not P2, and recognized whole rRBD (Figure 3). Likewise, anti-sera from mice immunized with peptide 2 (P2) recognized P2, but not P1 and recognized whole rRBD. Of note, neither anti-sera from P1- or P2-immunized mice were as reactive against rRBD as anti-sera from rRBD-immunized mice.

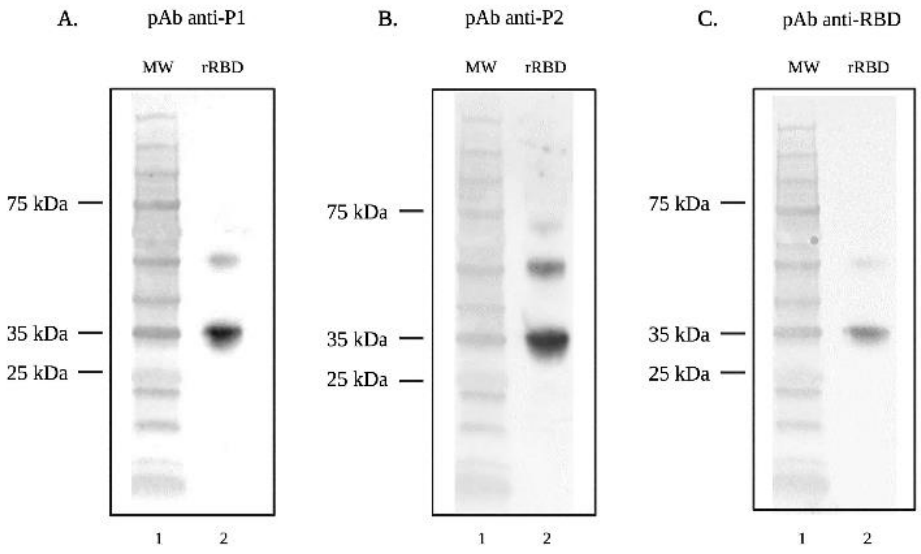

Figure 2. SDS-Page and Western blot analysis demonstrating recognition of SARS-CoV-2 (Wuhan) rRBD by anti-sera. Lane one for each Western blot contains the protein molecular weight marker. Lane two of each Western blot contains rRBD (37 kDa) probed with (A) pAb anti-P1, (B) pAb anti-P2, and (C) pAb anti-RBD followed by goat anti-mouse IgG-AP secondary antibody.

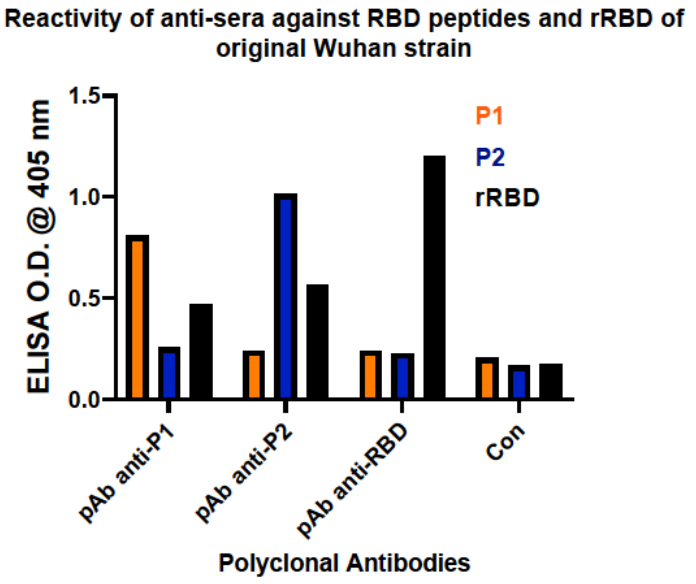

Figure 3. Enzyme-linked immunosorbent assay (ELISA) for reactivity of anti-sera against RBD peptides and rRBD of SARS-CoV-2 (Wuhan) Reactivity of anti-sera from mice immunized against P1, P2, and rRBD against whole rRBD and respective peptides.

Surrogate viral neutralization assay with anti-sera.

The three anti-sera samples from immunizations were used to determine if they contained antibodies that could neutralize the ability of RBD binding to ACE-2 using a commercially available surrogate viral neutralization assay kit. In this assay, HRP-labeled RBD is incubated with dilutions of anti-sera, and this mixture is added to plates coated with ACE-2. Data is recorded as percent signal inhibition. Only anti-sera from rRBD mice inhibited the binding of RBD to ACE-2, and this ability was at the maximal level detected by the kit (Figure 4).

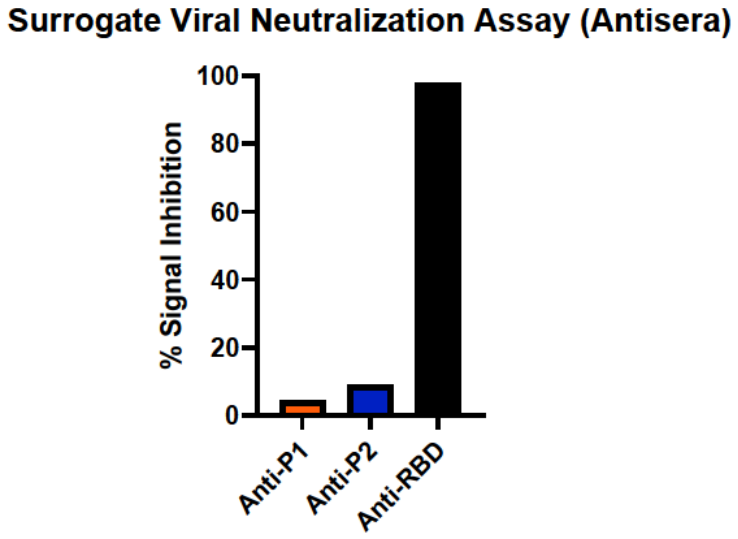

Figure 4. Surrogate Viral Neutralization Test (sVNT) demonstrating neutralization of RBD-ACE2 binding by anti-sera. Neutralization activity of anti-sera represented by percent signal inhibition of HRP-labeled RBD binding to ACE-2 by anti-sera from mice immunized against peptides P1, P2, and whole rRBD.

Characterization of monoclonal antibodies.

From immunizations and steps to develop cloned hybridomas secreting mAbs against P1, P2, and rRBD, three mAbs were cloned, isotyped, and named CU-P1-1 (IgG_1 κ) against P1, CU-P2-20 (IgG_1 κ) against P2, and CU-28-24 (IgG_{2b} κ) against rRBD. Using an ELISA approach to determine specificity, CU-P1-1 recognizes P1, but not P2, and slightly reacts with rRBD (Figure 5). CU-P2-20 recognizes the P2 peptide, but not P1, and is highly reactive against rRBD. CU-28-24 does not recognize either P1 or P2 but does react highly with rRBD. These hybridomas were then submitted to Kerafast, Inc. for sequencing to verify only one immunoglobulin gene (H + L) is expressed and the

correct isotype. Sequencing also provided the sequences for each of the six CDR regions responsible for epitope binding and are protected by non-disclosure agreements with Clemson University Research Foundation (CURF).

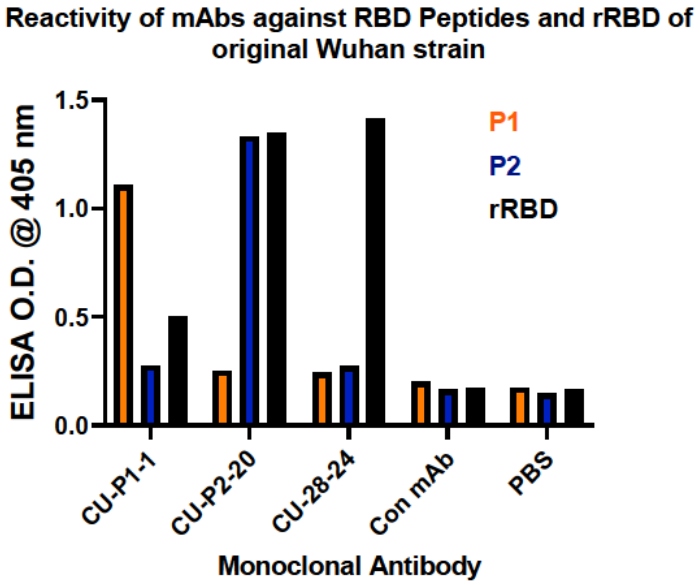

Figure 5. Enzyme-linked immunosorbent assay (ELISA) for reactivity of mAbs against RBD peptides and rRBD of SARS-CoV-2 (Wuhan). Reactivity of mAbs CU-P1-1, CU-P2-20, and CU-28-24 against P1, P2, and whole rRBD of original Wuhan strain of SARS-CoV-2

Each of the three mAbs was then tested by immunoblotting to verify the recognition of rRBD at the expected molecular weight. Monoclonal antibodies CU-P1-1 and CU-P2-20 recognize rRBD and recognize slight degradation products of the protein (Figure 6). However, mAb CU-28-24 does not recognize rRBD by immunoblotting, which is likely due to epitope destruction under the denaturing conditions of SDS-PAGE.

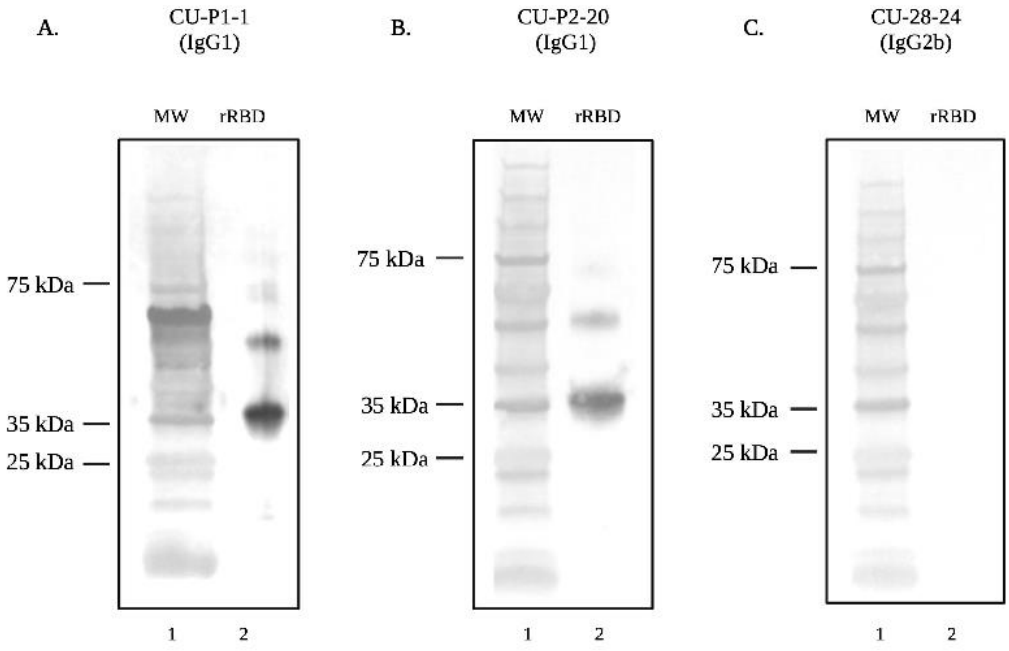

Figure 6. SDS-PAGE and Western blot analysis demonstrating recognition of rRBD of SARS-CoV-2 (Wuhan) by mAbs. Lane one for each Western blot contains the protein molecular weight marker. Lane two of each Western blot contains rRBD (Wuhan) probed with (A) mAb CU-P1-1, (B) mAb CU-P2-20, and (C) mAb CU-28-24 followed by goat anti-mouse IgG-AP secondary antibody.

Immunoprecipitation of rRBD with CU-28-24 and detection with CU-P2-20.

Efforts to immunoprecipitate rRBD with Protein-A/G bound CU-28-24 were successful in that after multiple washings of the bound column, rRBD was eluted from the column (Figure 7). FITC labeled CU-28-24 was then used to detect both eluted rRBD and pure rRBD by immunoblotting.

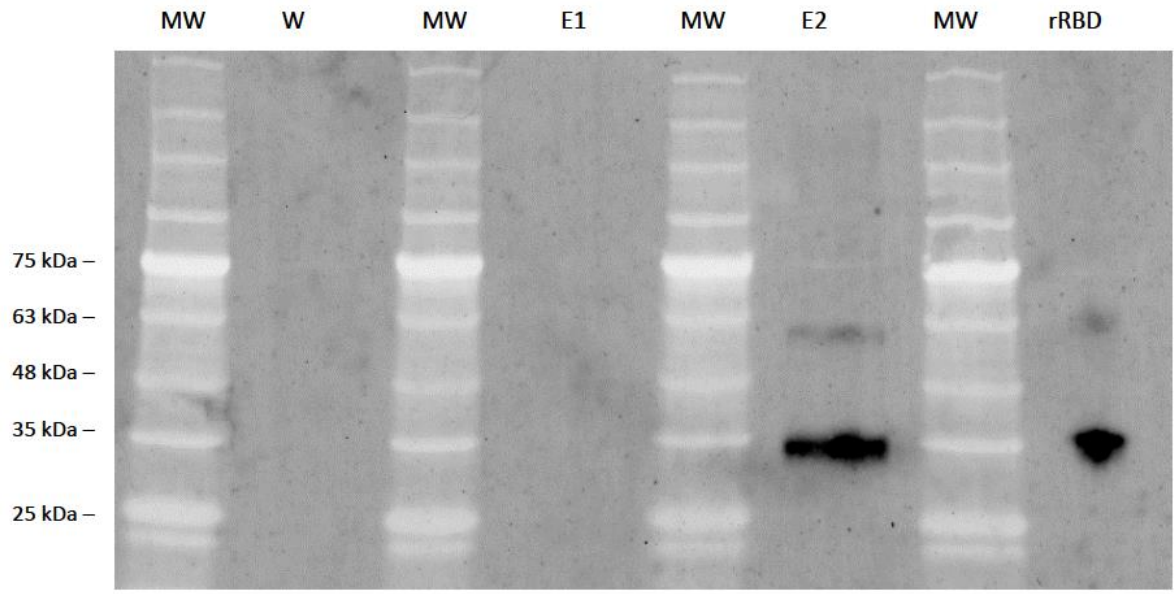

Figure 7. Immunoprecipitation of rRBD with mAb CU-28-24 and subsequent immunoblotting with mAb CU-P2-20. Purified mAb CU-28-24 was captured with protein A/G column, washed extensively, then rRBD was applied to the column to bind rRBD with mAb CU-28-24. After additional wash steps, the contents of the column were eluted in 1 ml fractions. The last wash step and first two elutions were subjected to SDS-PAGE and immunoblotting with FITC-labeled mAb CU-P2-20 and imaged. MW: molecular weight markers. rRBD: commercially sources rRBD as an internal control. Both precipitated and control rRBD were labeled.

Surrogate viral neutralization test with monoclonal antibodies.

Using the same commercially available platform used above for anti-sera, each of the three monoclonal antibodies were tested for their ability to neutralize the binding of labeled RBD to ACE-2. Both CU-P1-1 and CU-P2-20 lacked the ability to prevent RBD from binding to ACE-2, but CU-28-24 completely blocked this activity (Figure 8).

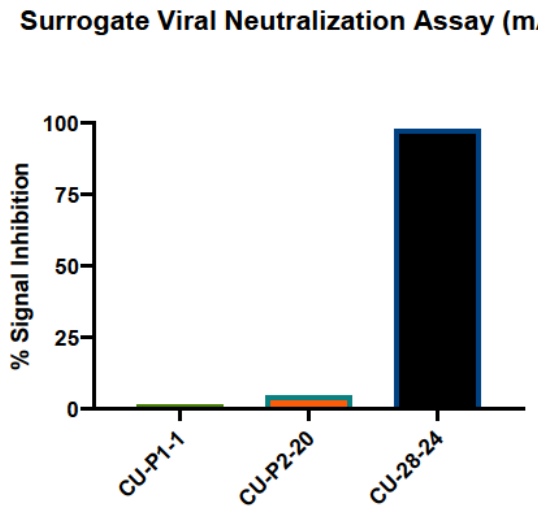

Figure 8. Surrogate Viral Neutralization Test (sVNT) demonstrating neutralization of RBD-ACE2 binding by mAbs. Neutralization activity represented as percent signal inhibition of HRP-labeled RBD binding to ACE-2 by mAbs CU-P1-1, CU-P2-20, and CU-28-24.

Plague reduction neutralization test using live SARS-CoV-2 virus.

The plaque reduction neutralization test is the gold standard for determining the neutralization titer of antibodies against live virus. Under the conditions carried out in the BSL-3 facility at Georgia State University, CU-P1-1 had no ability to block the virus from entering host Vero6 cells, and CU-P2-20 neutralized the virus with only a small titer of 4 (Figure 9). However, CU-28-24 had a $PRNT_{50}$ titer of 256.

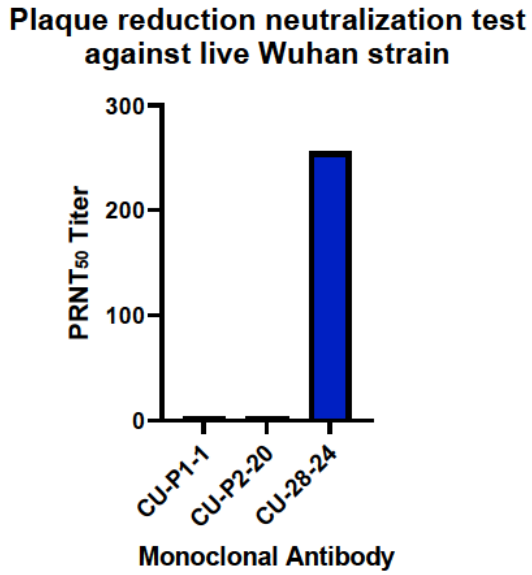

Figure 9. Plaque Reduction Neutralization Test of mAbs against live SARS-CoV-2 (Wuhan). Plaque Reduction Neutralization $Test_{50}$ titer of mAbs CU-P1-1, CU-P2-20, and CU-28-24 against live SARS-CoV-2 virus (Wuhan).

Immunohistochemistry using CU-P1-1, CU-P2-20, and CU-28-24.

Mouse tissues infected with SARS-CoV-2 (Wuhan) show intensive staining with mAbs CU-P2-20 and CU-28-24 (Figure 10). Alternatively, CU-P1-1 was only marginal in recognizing the virus in lung and brains, despite efforts to optimize conditions (images not shown). It was noted throughout optimization steps that antigen retrieval required a buffer of pH 9 for mAb CU-P2-20 and pH 6 for mAb CU-28-24.

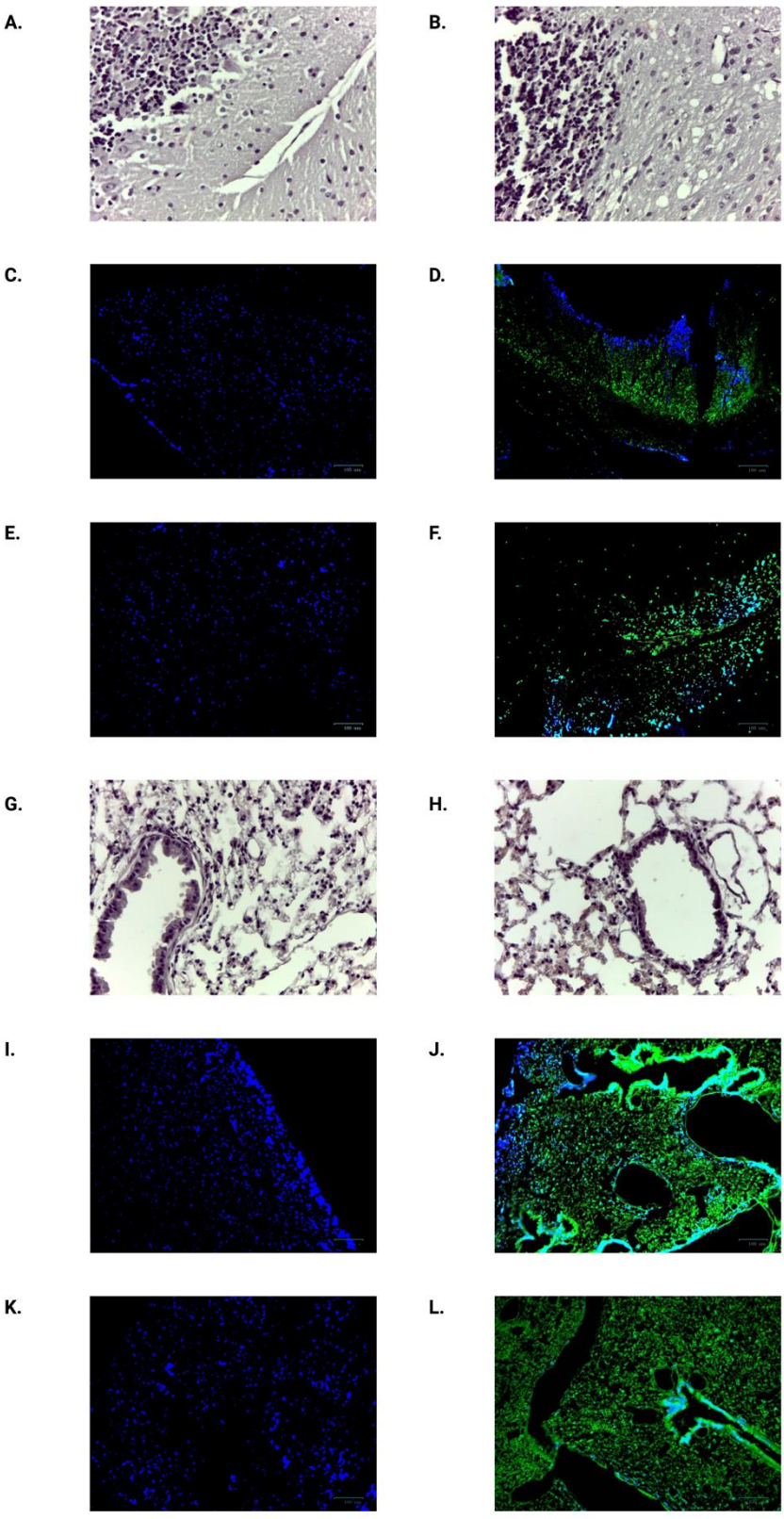
A.
B.
C.
D.
E.
F.
G.
H.
I.
J.
K.
L.

Figure 10. H&E staining and immunohistochemistry results of SAR-CoV-2 infected tissues with mAb CU-P2-20 and mAb CU-28-24. Tissues from either control or infected brains or lungs from SARS-CoV-2 (Wuhan strain) were H&E stained or were probed with mAbs, washed, then probed with FITC-labeled goat anti-mouse IgG and DAPI, washed and cover-slipped prior to imaging. (A) H&E staining of non-infected Brain (B) H&E staining of infected brain. (C) Non-infected brain: mab CU-28-24. (D) Infected brain: mAb CU-28-24. (E) Non-Infected Brain: mAb CU-P2-20. (F) Infected Brain: mAb P2-20. (G) H&E staining of non-infected lung. (H) H&E staining of infected lung. (I) Non-Infected Lung: mAb CU-28-24. (J) Infected lung: mAb CU-28-24. (K) Non-Infected Lung: mAb CU-P2-20. (L) Infected Lung: mAb CU-P2-20

Reactivity of mAbs against RBD of recent Omicron strains BA.2 and BA.4.5.

Recombinant RBD derived from Omicron strains BA.2 and BA.4.5. were used to coat ELISA plates and then probed with the three mAbs to compare reactivity with rRBD from the original Wuhan strain. CU-P1-1 and CU-P2-20 demonstrated relatively low reactivity against the two strains of Omicron tested in this study (Figure 11). As expected, each of these two were reactive against the rRBD from the Wuhan strain. CU-28-24, however, strongly recognized BA.2 and BA.4.5. rRBDs, as well as rRBD derived from the Wuhan strain.

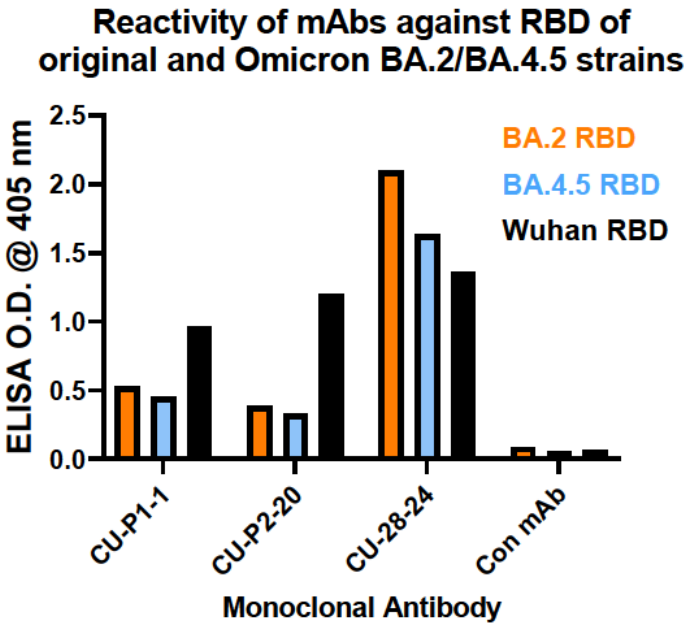

Figure 11. Enzyme-linked immunosorbent assay (ELISA) of reactivity of mAbs against rRBDs derived from SARS-CoV-2 (Wuhan) and Omicron variants BA.2 and BA.4.5. Reactivity of mAbs CU-P1-1, CU-P2-20, and CU-28-24 against RBD of original Wuhan strain and Omicron BA.2 and BA.4.5 variant strain RBDs.

DISCUSSION

In this study, a panel of three different monoclonal antibodies against non-overlapping epitopes within the RBD of the original Wuhan SARS-CoV-2 virus were successfully generated and characterized. Two of the three epitopes recognized by the panel are defined by the specific synthetic peptide (peptide 1 vs peptide 2) chosen for immunization, while the third antibody (CU-28-24) recognizes a yet to be determined epitope outside of the region of the two peptide sequences. The most common means to determine the epitope of mAb CU-28-24 would be peptide walking, in which overlapping synthetic peptides are generated to then screen the antibody by ELISA. Likewise, the peptide recognized by ELISA during the "walking" should also block the binding of CU-28-24 to whole rRBD in both ELISA and immunoblotting techniques. Based on the quality of mAb CU-28-24 as described below, future studies should be carried out to determine the specific epitope.

One of the many observations is that mAb CU-P2-20 reacts with P2 and rRBD equally well, but mAb CU-P1-1 against P1 does not bind well to rRBD in ELISAs. This observation may indicate that the region or epitope associated with P1 is not as immunogenic as predicted or is simply not available to the antibody in native full rRBD. Though Hopps & Woods hydrophilicity plotting, and NIH Abdesign programs predict P1 to be highly immunogenic, there may have been negative interactions between amino acids within the peptide that prevented the epitope to be fully expressed. For example, the original peptide designed by NIH Abdesign was AWNSNNLDSKVGGNYNYLYR, but this peptide is completely insoluble in water or PBS for immunizations. To make this

more soluble and suitable for immunization, the peptide was shortened to NSNNLDSKVGGNYNY prior to cysteine addition on the N-terminus for KLH conjugation. However, this sequence leads with asparagine (N) at the N-terminus, there are multiple N within the sequence, and two adjacent internal glycines (G), leading to the likelihood of hampered confirmational structure compared to the native rRBD [47]. Of note, mAb CU-P1-1 did recognize rRBD by SDS-PAGE/immunoblotting under reducing conditions, suggesting that the epitope within RBD may have been more readily revealed under these conditions. On the other hand, P2 (QTGKIADYNYKLPDDFTG) which was conjugated with KLH at the C-terminus using an additional cysteine and thus did not exhibit such predictable issues, was water soluble. Monoclonal antibody CU-P2-20, like mAb CU-P1-1, readily recognizes RBD in SDS-PAGE/immunoblotting and together with characteristics in ELISA mAb CU-P2-20 should have applications in a variety of endpoints. Of note, based on the amino acid sequence of the RBDs of SARS-CoV and SARS-CoV-2, mAb CU-P1-1 may distinguish between the two and mAb CU-P2-20 should have activity against both.

The observation that mAb CU-28-24 recognizes RBD by ELISA, but not by SDS-PAGE/immunoblotting indicates that its specific epitope is destroyed during the denaturing conditions. However, this does not hinder the ability of the antibody to immunoprecipitate rRBD for recognition by CU-P2-2-, nor does it hinder the ability of the antibody to neutralize the live virus in PRNT assays and inhibit binding of labeled RBD to ACE-2 in surrogate PRNTs. Therefore, this antibody should be of high value in future studies with other strains (variants of concern). To that end, mAb CU-28-24

readily recognizes rRBDs from the Omicron BA.2 variant and the BA.4/BA.5 variant, and the degree of response in ELISA was comparable to activity against rRBD from the original Wuhan strain. Future studies with CU-28-24 should be conducted to determine if current variants of concern and those appearing in the future are neutralized by this antibody. In this regard, mAb CU-P1-1 and mAb CU-P2-20 have no value in terms of viral neutralization.

As mentioned in my Introduction section, anti-viral antibodies may have several functions outside of the ability to neutralize a virus of concern. One endpoint of high value with mAbs is in immunohistochemistry for detecting the virus in specific tissues. Using IHC and immunofluorescent labeled secondary antibody, it seems that CU-P1-1 does not work well for IHC. However, mAbs CU-P2-20 and CU-28-24 show viral infection in infected lungs and brains of mice exposed to the virus, and this activity seems to be concentrated in focal regions, consistent with observations made by others [48-50]. While some studies use antibodies generated against nucleocapsid proteins [51, 52], many others use antibodies against the RBD [53]. Of concern would be the high rate of mutation within the RBD of variants of concern post emergence of the Wuhan strain, making some original RBD-based antibodies ineffective. However, based on the ELISA results against Omicron BA.2 and BA.4.4, mAb CU-28-24 should be a good reagent going forward.

My original hypothesis was that defined synthetic peptides derived from the RBD region of the SARS-CoV-2 virus would be a viable approach to developing high quality antibodies with a broad range of applications. Considering the importance of

neutralizing antibodies for possible therapeutic endpoints, this hypothesis seems wrong and larger proteins for immunization would be best, as demonstrated by mAb CU-28-24. However, a panel of only three mAbs is not enough to make broad statements about the utility of peptide-based immunogens compared to larger, more native proteins from which the peptide sequences were derived. Regardless, this study provides at least two very good mAbs for continued research related to COVID-19 and the emerging variants of concern. Considering the high degree of cross-reactivity of mAb CU-28-24 with Omicron variants BA.2 and BA.4.5, it may be useful in clinical settings, especially if the antibody were to be humanized. In this case, the mouse nucleic acids corresponding to the six CDR regions would be grafted into a human IgG immunoglobulin molecule and expressed as a recombinant protein in CHO cells.

CONCLUSION

Despite the successes with the development of vaccines, anti-viral drugs, and monoclonal antibodies for the treatment of SARS-CoV-2 and its many evolved variants of concern, there is still a need for high-quality monoclonal antibodies. This is especially true for variants of concern, such as the current Omicron variants, that are resistant to earlier monoclonals targeted against the original Wuhan strain. I believe my three antibodies, especially mAb CU-P2-20 and mAb CU-28-24, will have both research and clinical applications in the future. All three hybridomas have been sequenced, thereby allowing scientists to express these valuable mAbs as recombinant proteins. This will supplant the need for careful and laborious hybridoma maintenance going forward. The

hybridomas/mAbs are under Intellectual Property protection by the Clemson University Research Foundation, and the three CDRs have been submitted as a pending patent.

REFERENCES

1. Cui, J., F. Li, and Z.L. Shi, *Origin and evolution of pathogenic coronaviruses.* Nat Rev Microbiol, 2019. **17**(3): p. 181-192.

2. Fehr, A.R. and S. Perlman, *Coronaviruses: an overview of their replication and pathogenesis.* Methods Mol Biol, 2015. **1282**: p. 1-23.

3. Chen, B., et al., *Overview of lethal human coronaviruses.* Signal Transduct Target Ther, 2020. **5**(1): p. 89.

4. Huang, Y., et al., *Structural and functional properties of SARS-CoV-2 spike protein: potential antivirus drug development for COVID-19.* Acta Pharmacol Sin, 2020. **41**(9): p. 1141-1149.

5. Payne, S., *Family Coronaviridae*, in *Viruses*. 2017. p. 149-158.

6. Yadav, R., et al., *Role of Structural and Non-Structural Proteins and Therapeutic Targets of SARS-CoV-2 for COVID-19.* Cells, 2021. **10**(4).

7. Lim, Y.X., et al., *Human Coronaviruses: A Review of Virus-Host Interactions.* Diseases, 2016. **4**(3).

8. Ye, Z.W., et al., *Zoonotic origins of human coronaviruses.* Int J Biol Sci, 2020. **16**(10): p. 1686-1697.

9. Zhu, Z., et al., *From SARS and MERS to COVID-19: a brief summary and comparison of severe acute respiratory infections caused by three highly pathogenic human coronaviruses.* Respir Res, 2020. **21**(1): p. 224.

10. Abdelrahman, Z., M. Li, and X. Wang, *Comparative Review of SARS-CoV-2, SARS-CoV, MERS-CoV, and Influenza A Respiratory Viruses.* Front Immunol, 2020. **11**: p. 552909.

11. Zumla, A., D.S. Hui, and S. Perlman, *Middle East respiratory syndrome.* Lancet, 2015. **386**(9997): p. 995-1007.

12. *MERS situation update: December 2022*, W.H. Organization, Editor. 2022: Regional Office for the Eastern Mediterranean.

13. Memish, Z.A., et al., *Middle East respiratory syndrome.* Lancet, 2020. **395**(10229): p. 1063-1077.

14. Chafekar, A. and B.C. Fielding, *MERS-CoV: Understanding the Latest Human Coronavirus Threat.* Viruses, 2018. **10**(2).

15. Azhar, E.I., et al., *The Middle East Respiratory Syndrome (MERS).* Infect Dis Clin North Am, 2019. **33**(4): p. 891-905.

16. Wang, M.Y., et al., *SARS-CoV-2: Structure, Biology, and Structure-Based Therapeutics Development.* Front Cell Infect Microbiol, 2020. **10**: p. 587269.

17. Rana, R., et al., *A Comprehensive Overview on COVID-19: Future Perspectives.* Front Cell Infect Microbiol, 2021. **11**: p. 744903.

18. Uddin, M., et al., *SARS-CoV-2/COVID-19: Viral Genomics, Epidemiology, Vaccines, and Therapeutic Interventions.* Viruses, 2020. **12**(5).

19. *Weekly Epidemiological Update on COVID-19 - 16 March 2023*. 2023, World Health Organization.

20. Cevik, M., et al., *Virology, transmission, and pathogenesis of SARS-CoV-2.* BMJ, 2020. **371**: p. m3862.

21. Harrison, A.G., T. Lin, and P. Wang, *Mechanisms of SARS-CoV-2 Transmission and Pathogenesis.* Trends Immunol, 2020. **41**(12): p. 1100-1115.

22. Hu, B., et al., *Characteristics of SARS-CoV-2 and COVID-19.* Nat Rev Microbiol, 2021. **19**(3): p. 141-154.

23. Ma, Q., et al., *Global Percentage of Asymptomatic SARS-CoV-2 Infections Among the Tested Population and Individuals With Confirmed COVID-19 Diagnosis: A Systematic Review and Meta-analysis.* JAMA Netw Open, 2021. **4**(12): p. e2137257.

24. *Coronavirus Disease 2019 (COVID-19) Treatment Guidelines*. National Institutes of Health.

25. Jackson, C.B., et al., *Mechanisms of SARS-CoV-2 entry into cells.* Nat Rev Mol Cell Biol, 2022. **23**(1): p. 3-20.

26. Gruell, H., et al., *Antibody-mediated neutralization of SARS-CoV-2.* Immunity, 2022.

27. Singh, S., et al., *How an outbreak became a pandemic: a chronological analysis of crucial junctures and international obligations in the early months of the COVID-19 pandemic.* The Lancet, 2021. **398**(10316): p. 2109-2124.

28. Najjar-Debbiny, R., et al., *Effectiveness of Paxlovid in Reducing Severe Coronavirus Disease 2019 and Mortality in High-Risk Patients.* Clinical Infectious Diseases, 2022. **76**(3): p. e342-e349.

29. Najjar-Debbiny, R., et al., *Effectiveness of Molnupiravir in High-Risk Patients: A Propensity Score Matched Analysis.* Clinical Infectious Diseases, 2023. **76**(3): p. 453-460.

30. Butler, C.C., et al., *Molnupiravir plus usual care versus usual care alone as early treatment for adults with COVID-19 at increased risk of adverse outcomes (PANORAMIC): an open-label, platform-adaptive randomised controlled trial.* The Lancet, 2023. **401**(10373): p. 281-293.

31. Cao, Z., et al., *VV116 versus Nirmatrelvir–Ritonavir for Oral Treatment of Covid-19.* New England Journal of Medicine, 2022. **388**(5): p. 406-417.

32. Ganatra, S., et al., *Oral Nirmatrelvir and Ritonavir in Nonhospitalized Vaccinated Patients With Coronavirus Disease 2019.* Clinical Infectious Diseases, 2022. **76**(4): p. 563-572.

33. Voss, W.N., et al., *Prevalent, protective, and convergent IgG recognition of SARS-CoV-2 non-RBD spike epitopes.* Science, 2021. **372**(6546): p. 1108-1112.

34. Piccoli, L., et al., *Mapping Neutralizing and Immunodominant Sites on the SARS-CoV-2 Spike Receptor-Binding Domain by Structure-Guided High-Resolution Serology.* Cell, 2020. **183**(4): p. 1024-1042.e21.

35. Dejnirattisai, W., et al., *The antigenic anatomy of SARS-CoV-2 receptor binding domain.* Cell, 2021. **184**(8): p. 2183-2200.e22.

36. Hwang, Y.-C., et al., *Monoclonal antibodies for COVID-19 therapy and SARS-CoV-2 detection.* Journal of Biomedical Science, 2022. **29**(1): p. 1.

37. Planas, D., et al., *Resistance of Omicron subvariants BA.2.75.2, BA.4.6, and BQ.1.1 to neutralizing antibodies.* Nat Commun, 2023. **14**(1): p. 824.

38. Wang, X., et al., *Concerns on Bebtelovimab (LY-CoV1404) used to neutralize Omicron subvariants.* J Med Virol, 2023. **95**(2): p. e28565.

39. Burton, D.R., *Antibodies, viruses and vaccines.* Nature Reviews Immunology, 2002. **2**(9): p. 706-713.

40. Rice, C.D., et al., *Cross-reactivity of monoclonal antibodies against peptide 277–294 of rainbow trout CYP1A1 with hepatic CYP1A among fish.* Mar Environ Res, 1998. **46**(1–5): p. 87-91.

41. Margiotta, A.L., L.J. Bain, and C.D. Rice, *Expression of the Major Vault Protein (MVP) and Cellular Vault Particles in Fish.* The Anatomical Record, 2017. **300**(11): p. 1981-1992.

42. Marsh, M.B. and C.D. Rice, *Development, characterization, and technical applications of a fish lysozyme-specific monoclonal antibody (mAb M24-2).* Comparative Immunology, Microbiology and Infectious Diseases, 2010. **33**(6): p. e15-e23.

43. Margiotta, A. and B.H. Gray, *Assessment of recurrent mesenteric ischemia after stenting with a pressure wire.* Vascular Medicine, 2014.

44. The, T.H. and T.E. Feltkamp, *Conjugation of fluorescein isothiocyanate to antibodies. I. Experiments on the conditions of conjugation.* Immunology, 1970. **18**(6): p. 865-73.

45. Bewley, K.R., et al., *Quantification of SARS-CoV-2 neutralizing antibody by wild-type plaque reduction neutralization, microneutralization and pseudotyped virus neutralization assays.* Nature Protocols, 2021. **16**(6): p. 3114-3140.

46. Kumari, P., et al., *Neuroinvasion and Encephalitis Following Intranasal Inoculation of SARS-CoV-2 in K18-hACE2 Mice.* Viruses, 2021. **13**(1).

47. Lee, B.S., et al., *Antibody Production with Synthetic Peptides.* Methods Mol Biol, 2016. **1474**: p. 25-47.

48. Best Rocha, A., et al., *Detection of SARS-CoV-2 in formalin-fixed paraffin-embedded tissue sections using commercially available reagents.* Laboratory Investigation, 2020. **100**(11): p. 1485-1489.

49. Sun, Y., et al., *Sensitive and Specific Immunohistochemistry Protocol for Nucleocapsid Protein from All Common SARS-CoV-2 Virus Strains in Formalin-Fixed, Paraffin Embedded Tissues.* Methods and Protocols, 2021. **4**(3): p. 47.

50. Lonardi, S., et al., *Immunohistochemical Detection of SARS-CoV-2 Antigens by Single and Multiple ImmunohistochemistryImmunohistochemistry (IHC)*, in *SARS-CoV-2: Methods and Protocols*, J.J.H. Chu, B.A. Ahidjo, and C.K. Mok, Editors. 2022, Springer US: New York, NY. p. 291-303.

51. Colson, A., et al., *Clinical and in Vitro Evidence against Placenta Infection at Term by Severe Acute Respiratory Syndrome Coronavirus 2.* Am J Pathol, 2021. **191**(9): p. 1610-1623.

52. Mustroph, J., et al., *Cardiac Fibrosis Is a Risk Factor for Severe COVID-19.* Front Immunol, 2021. **12**: p. 740260.

53. Saccon, T.D., et al., *SARS-CoV-2 infects adipose tissue in a fat depot- and viral lineage-dependent manner.* Nat Commun, 2022. **13**(1): p. 5722.